Adsorption of T.N.T. from Wastewater Using Ni-Oxide and Cu-Oxide Nanoparticles

Amal A. Altalhi [1], Salwa M. Morsy [2], Seham A. Shaban [2] and Sahar M. Ahmed [2]

[1] Chemistry department, College of Science, Taif University, P.O. Box 1109, Taif 21944, Saudi Arabia

[2] Egyptian Petroleum Research Institute, Nasr City, Cairo, Egypt

Abstract: Nanocrystalline nickel oxide (NiO) and copper oxide (CuO) have been synthesized in a water-in-oil microemulsion. The as-synthesized samples were characterized by X-ray diffraction (XRD), Electron Spin Resonance (E.S.R.), transmission electron microscopy (T.E.M.), and Specific Surface Area (S.S.A.). The particle size of nickel oxide and copper oxide can be controlled from 10.0 to 21.5 and 12.5 to 25.0 nm, respectively, at a different time of calcination temperature with a fixed proportion of water, surfactant, and oil in the microemulsion. Also, the results showed that the specific surface area (89.96 m^2 g^{-1}) and pore diameter (8.11 nm) of the prepared nano NiO are higher than the specific surface area (71.96 m^2 g^{-1}) and pore diameter (3.71 nm) of the prepared nano CuO. An adsorption test was carried out to show the efficiency of these prepared NiO and CuO nanoparticles for the Adsorption of T.N.T. in an aqueous solution. The removal efficiencies of both nano NiO and CuO were achieved at 90.06% and 77.0%, respectively.

Additionally, NiO and CuO nanoparticles were regenerated for five cycles. The Kinetic models of Pseudo first-order and pseudo-second-order were described. The results demonstrated that T.N.T. adsorption on both nano adsorbents follows the pseudo-second-order model.

Keywords: nano adsorbents; nickel oxide; copper oxide; microemulsion; T.N.T. adsorption.

1. Introduction

Wastewater is a global concern. It directly impacts the biological diversity of aquatic ecosystems, disrupting the fundamental integrity of our life support systems on which a wide range of sectors from urban development to food production and industry depend [1-3]. One explosive that is widely used for military and civil purposes all over the world is 2,4,6-trinitrotoluene (T.N.T.) [4]. As a result of this ubiquitous use, residual T.N.T. in both soil and groundwater have been detected [5,6]. Thus, T.N.T. has been listed as a significant pollutant to public health and aquatic life by the USEPA [7]. Different methods, such as catalysis, photocatalysis, and adsorption have been used to eliminate contamination from wastewater [8-16].

It is important to develop low-cost and effective technology for the removal of waste explosives precisely T.N.T. So, several methods have been used for decontamination of T.N.T. from wastewater and contaminated soil such as biotreatment [17], alkaline hydrolysis, chemical reduction, catalytic degradation, photocatalytic degradation**,** flocculation, and adsorption [18-27]. High surface area and low-cost adsorbents are often favored to eliminate harmful materials [28]. The use of nanoparticles as adsorbents has recently drawn great interest because of their higher surface area and higher porosity, contributing to preferred adsorption characteristics [29]. The most significant materials, nickel oxide (NiO) and copper oxide (CuO) have high chemical stability unique magnetic properties. In the adsorption of heavy metals and organic dyes [30,31], CuO and NiO were investigated as metal oxide nano-adsorbents [32-35]. However, it is interesting to note that the studies on the Adsorption of T.N.T. using nanoscale metal oxides are still limited. Therefore, this paper aims to prepare and evaluate nickel oxide and copper oxide nanoparticles' performance as adsorbents for removing T.N.T. from aqueous solutions. The prepared nano adsorbents were characterized by X-ray diffraction, Transmission Electron Microscopy (T.E.M.), Electron Spin Resonance Technique (E.S.R.), and Specific Surface Area (S.S.A.). The adsorption performance of nickel oxide and copper oxide nanoparticles was examined. The adsorption kinetics and reusability of the prepared adsorbents were studied.

2. Experimental

2.1. Materials

Cetyl trimethyl ammonium bromide as cationic surfactant (C9H13N Br), nickel chloride hexahydrate (99.9%), and copper chloride dihydrate (purity 99.2%) were supplied from Sigma-Aldrich U.S.A., n-hexane, n-butanol, were purchased from Sinopharm Chemical Reagent Co., Ltd., Chinese. 2,4,6-trinitrotoluene (T.N.T.) was obtained from the Factory-18 (Abou-Zaabal, Cairo, Egypt).

2.2. Synthesis of nickel oxide and copper oxide nanoparticles by the microemulsion method

A representative synthesis of the copper and nickel oxide nanoparticles involved the mixing of two reverse microemulsions. The first microemulsion was prepared by taking 25 mL of 0.1 M solution of cetyl trimethyl ammonium bromide in n-hexane and adding 300 µL of n-butanol (co-surfactant) and 225 µL of a 5% (w/v) aq. solution of nickel chloride or copper chloride. The second microemulsion was prepared as the same procedure, but nickel or copper chlorides were replaced by alkaline sodium carbonate solution. Both the microemulsions were left stirring at 500 rpm for 30 minutes to obtain an optically clear homogeneous dispersion. Nickel or copper basic carbonates nanoparticles were formed by mixing the two microemulsions' appropriate volumes with vigorous stirring at 500 rpm for 30 min. The precipitates were washed with ethanol and distilled water to remove the undesirable contaminants. The washed precipitates were dried and then calcined at 400ºC for one and two hrs. to obtain the corresponding metal oxide nanoparticles [36].

2.3. Adsorption experiments (Batch reactor)

Batch tests were completed on a condition that specific concentrations of Ni-oxide and Cu-oxide nanoparticles were applied to reduce 100 mg/l of T.N.T. stock solutions. The solutions were processed on a rotary shaker (150 rpm) at room temperature for 2 hours. The solution was centrifuged, and the mother liquor was analyzed for residual T.N.T. concentration with HPLC. The following equation was used to determine the

$$q_e = (C_o - C_e) \times V/W$$

Where q_e is the adsorption capacity (mg g-1) in the solid at equilibrium; C_o and C_e are the initial and equilibrium concentrations of metals/contaminant (mg L^{-1}) respectively; V is the volume of the aqueous solution; W is the mass (g) of adsorbent used in the experiments [37]. Adsorption experiments were performed at least three times to examine the results' repeatability and verify experimental data.

2.4. Reusability Experimental

The reusability of the prepared nano-CuO and nano-NiO was tested by performing five alternating adsorption-desorption cycles. The collected adsorbents were then dispersed into 20 mL of 0.5-M HCl and shaken at 180 rpm for 10 minutes to regenerate the adsorbent. Before the next cycle, the regenerated adsorbent was washed repeatedly with ultrapure water until the effluent was neutral (pH 7). The regenerated NiO and CuO were used for sequential adsorption-desorption cycles and the T.N.T. adsorption efficiency were obtained.

2.5. Instruments

2.5.1. X-ray diffraction (XRD) X-ray diffraction
patterns were recorded on a P.A.N. analytical X'Pert PRO instrument with Cu Kα (1.54 Å) radiation at 40kV and 40 mA in the range of 2θ= 10-80º.

2.5.2. Transmission Electron Microscopy (T.E.M.)
The catalysts' microstructures were examined by transmission electron microscopy (T.E.M.) on a JEOL JEM -2000EX at an accelerating voltage of 100kV.

2.5.3. Electron Spin Resonance Technique (E.S.R.)
The ESR-spectra were recorded on a Brucker, Elex-500 spectrometer with the ER-4131VT variable temperature accessory at room temperature and liquid nitrogen temperature. The spectrometer was operated at X-band frequency, and the samples were held on a silica tube.

2.5.4. Specific Surface Area (S.S.A.)
The average particle size and Specific Surface Area of the catalyst samples prepared were determined on a Quantachrome 3200.

2.5.5. High-performance liquid chromatography (HPLC)
The concentration of T.N.T. was determined by Agilent HPLC 1260 infinity series (Agilent Technologies) equipped with a quaternary pump, a variable wavelength diode array detector (D.A.D.).

3. Results and Discussion

3.1. Adsorbents Characterization
X-ray diffraction (XRD) analysis of the prepared Ni- and Cu-oxides thermally treated at 400ºC for one and two hours are shown in Figs. 1,2. The characteristic diffraction peaks corresponded to (111), (200), (220), (202), (311), and (222) indicate the monoclinic structure of NiO and CuO nanocrystals, which were also found to be highly crystalline planes of NiO and CuO. The observed interplanar spacing, d hkl, was compared with the data of JCPDS card number of 78-0429 for NiO and JCPDS 45-0937 for CuO. The results obtained in this study are further supported by XRD results obtained for NiO [38,39] and CuO nanoparticles [40,41]. XRD patterns for Ni-oxide preheated for 1 hr are less intensive compared with oxide calcined for 2 hr. This may be ascribed to the increase of particle size upon prolonged calcination Table 1. The average particle size of each crystalline oxides Table 1 was determined according to the Scherrer formula: **d = 0.89/b cos θ,** where d is the average particle size and b stands for the full-width at half-height of the peaks.
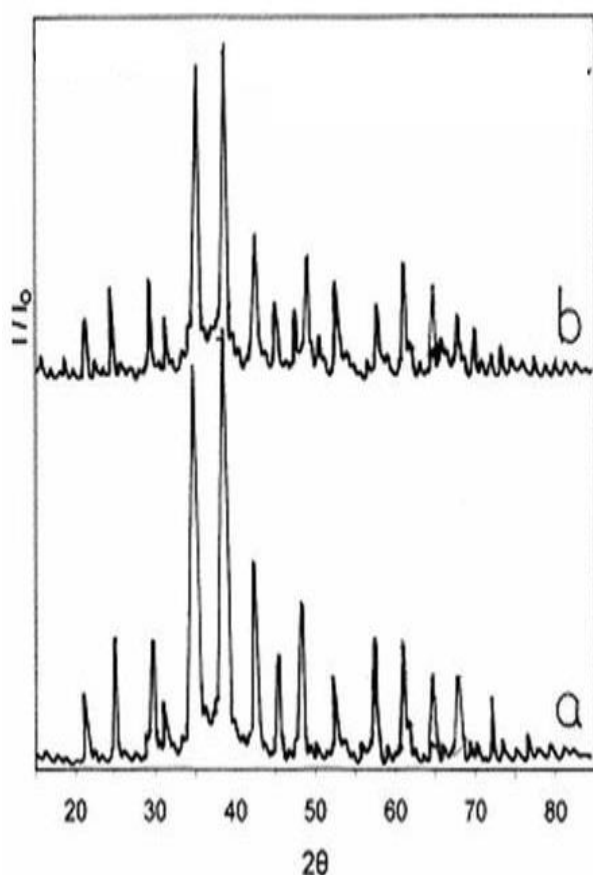
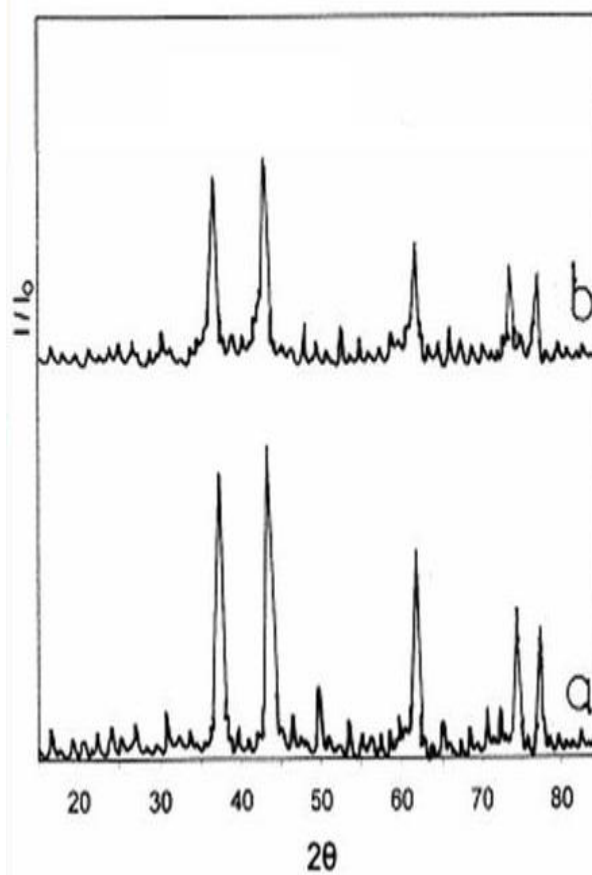**Figure 1**. X-ray diffraction of nickel oxide nanoparticle calcined at a different time for two hr. (a) and one hr. (b)

Figure 2. X-ray diffraction of copper oxide nanoparticle calcined at a different time for two hr. (a) and one hr. (b)

Table 1. The particle size and surface area of nickel oxide and copper oxide nanoparticles calcined at different time.

Metal oxide	Particle Size, nm		Surface Area, cc/g		Pore diameter, nm	
	1hr.,400ºC	2hr,400ºC	1hr.,400ºC	2hr.,400ºC	1hr.,400ºC	2hr.,400ºC
NiO	10	21.5	89.96	41.84	8.11	3.71
CuO	12.5	25	71.96	35.98	7.24	3.67

Table 1 reveals that the particle size of the oxide prepared via microemulsion technique is considerably increased by increase calcination temperature. Prolonged heating of the solid is associated with a pronounced increase of the particle size, probably due to heat and mass transfer during calcination.

3.2. The textural properties
Specific surface areas and porosity of the prepared nanometal oxides were examined by N_2 adsorption-desorption measurements performed at 77K. The corresponding adsorption-desorption isotherms are shown in Fig. 3. Both the nano-NiO and nano-CuO gave similar nitrogen adsorption-desorption isotherms. They corresponded to type II of the IUPAC classification and showed a characteristic hysteric's loop associated with capillary condensation in mesopores Fig. 3 [42].
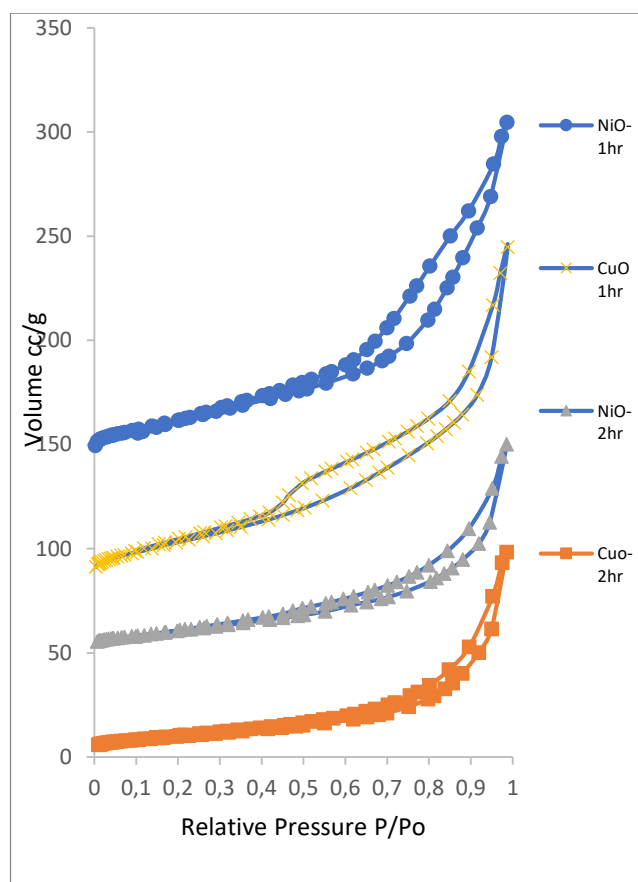
Figure 3. Nitrogen adsorption-desorption isotherms of nickel oxide and copper oxide nanoparticles calcined at different times for one and two hours
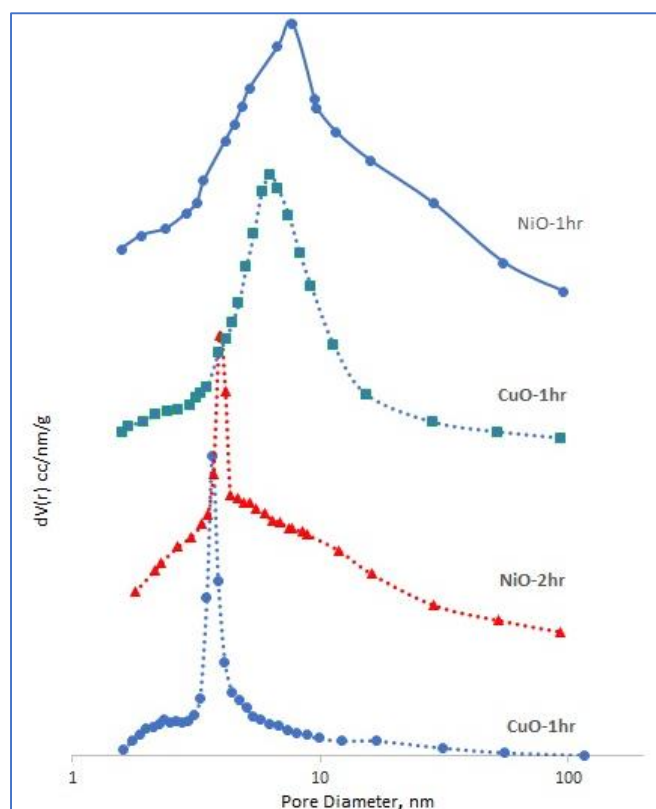
Figure 4. Pore diameter of nickel oxide and copper oxide nanoparticles calcined at different times for one and two hours

3.3. Transmission Electron Microscopy

(T.E.M.) Figs. 4,5 illustrate the photographs of the investigated samples prepared by the microemulsion technique. Figs. 4,5 depict that; smaller particle sizes characterize the prepared oxides calcined at 400°C for 1 hr than their equivalents calcined for 2 hr. The synthesized NiO N.P.s were flakes nano rod-like

structures with tiny agglomerates and sizes of (4 - 10 nm). Meanwhile, the CuO N.P.s were mostly cubic with size ranged (10 -25 nm), as confirmed by XRD. So, the particle size of CuO is relatively larger than the particle size of NiO, prepared under the same conditions.
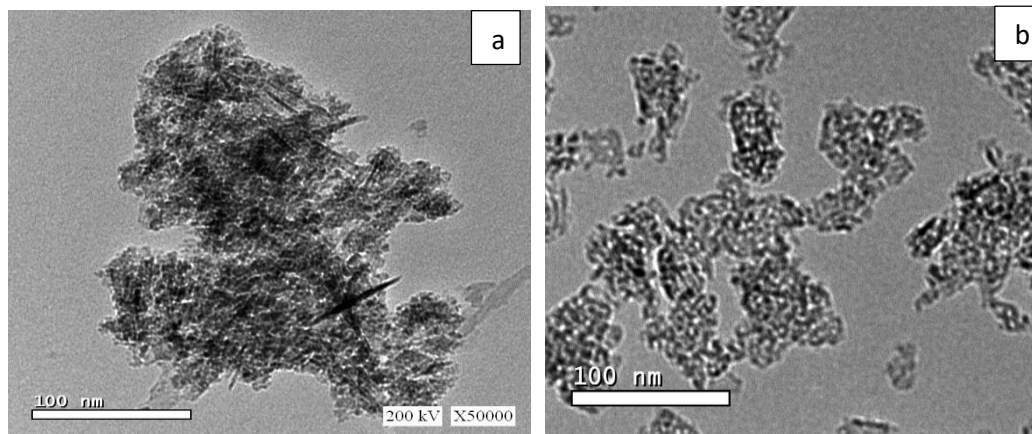

Figure 5. T.E.M. of nickel oxide nanoparticle calcined at different times for one hour (a) and (b) two hours
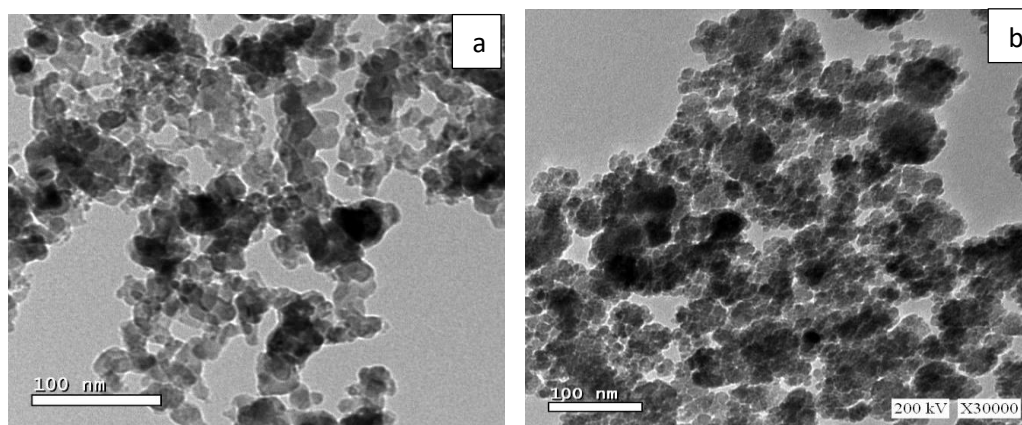

Figure 6. T.E.M. of copper oxide nanoparticle calcined at different times for one hour (a) and (b) two hours

A progressive decrease in the amount of the adsorbed N_2, i.e., a reduction in surface area, is observed with an increase in calcination time, according to Table 1. Additionally, an apparent type-H4 hysteresis loop can also be seen in the relative vapor pressure range of 0.4–1.0 bar, indicating the presence of a mesoporous system Fig. 4 [43]. The B.E.T. surface area and pore diameter of the adsorbents are summarized in Table 1. It can be found that the B.E.T. specific surface of the prepared nano NiO decreases from 89.96 m^2 g^{-1} to 41.84 m^2 $g^{-1}$by increasing of time of calcination from 1h to 2h while the B.E.T. of the CuO decrease from 71.96 to 35.98 m^2 g^{-1}. The Pore diameter is gradually decreased from 8.11, 3.71 to 3.71, 3.67 nm for NiO and CuO, respectively, with the increase of calcination time from 1 hr to 2 hr at 400°C. The higher surface area of NiO may be due to the smaller pore diameter. The vast majority of the total surface area and pore diameter of all samples were emanated from mesopores. Such mesoporous structure would be propitious for adsorption purposes in terms of

improved accessibility of the adsorbent to the active binding centers within the porous structure of samples, ubiquitous existence in effluents worldwide, extreme toxicity and hazardous nature towards many living creatures, high water solubility, and increased persistence in aquatic ecosystems [44,45].

3.4. Electron Spin Resonance (E.S.R.)

E.S.R. spectra of the investigated samples are presented in Figs. 7,8. The E.S.R. spectra of NiO prepared by microemulsion method Fig. 7 showed moderately sharp isotropic for the oxide calcined for 2 hr and strong isotropic signal for NiO calcined for 1 hr. The strong isotropic signal that appeared for the sample prepared by microemulsion (calcined for 1 hr) may be related to the presence of trivalent nickel or/and the formation of nano Ni-oxide particles. This strong signal can be attributed to the superparamagnetic effect detectable in nanoparticles with high magnetic property [46]. The E.S.R. spectra of Cu-oxide Fig. 8 prepared by microemulsion calcined

for 1 hr show a sharp isotropic signal indicating the formation of nanoparticles of Cu-oxide, while the E.S.R. spectra of Cu-oxide calcined at 400°C for 2hr show moderately sharp isotropic for the oxide indicating that the investigated solid exhibits

diamagnetic properties [47,48]. In general, E.S.R. of CuO and NiO calcined for one and two hours show strong and moderately sharp isotropic signals, respectively, indicating differences in the magnetic properties.
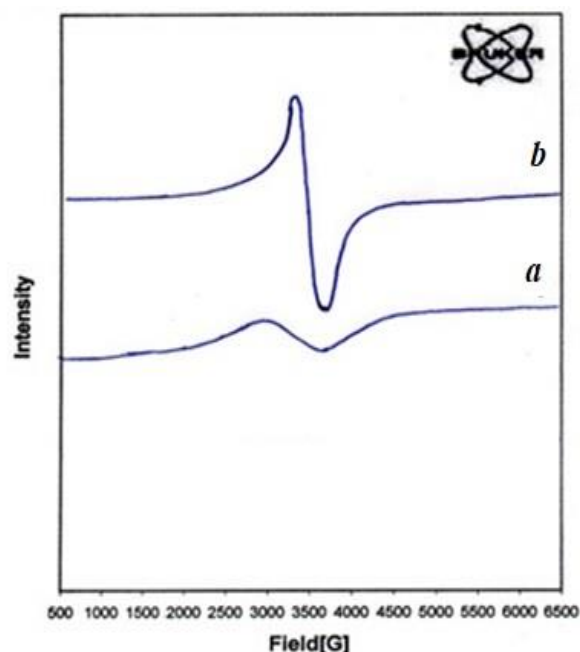

Figure 7. E.S.R. of nickel oxide nanoparticle calcined at different times for two hours (a) and one hour (b)
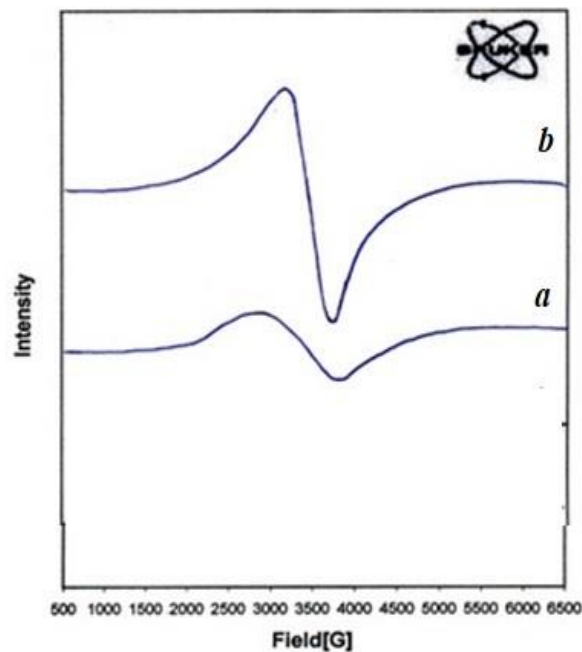

Figure 8. E.S.R. of copper oxide nanoparticle calcined at different times for two hours (a) and one hour (b)

3.5. Comparison of T.N.T. adsorption using Nickel and Copper Oxide Nanoparticles

As shown in Figs. 9,10, the adsorption process of T.N.T. by nickel oxide and copper oxide nanoparticles was rapid in the first 60 min with percentage removal of 90.6 %, and 77.2% reaches

its maximum value (94.5%) and 87.5% after 120 min for nickel and copper oxides, respectively. The higher efficiency of NiO can be attributed to its high surface area. Further increase in the contact time did not affect the adsorption.
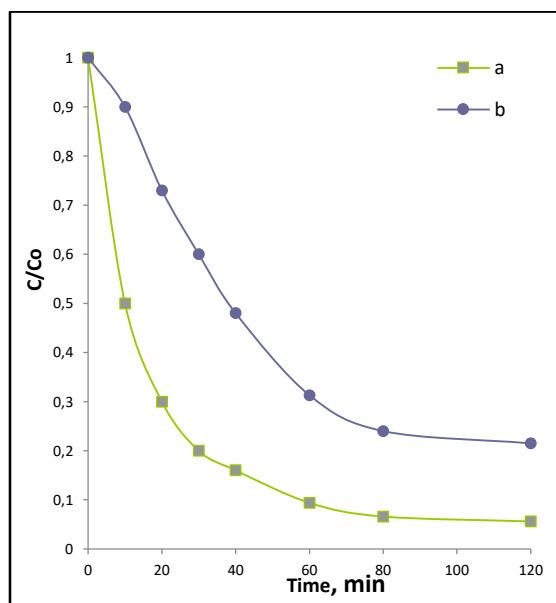

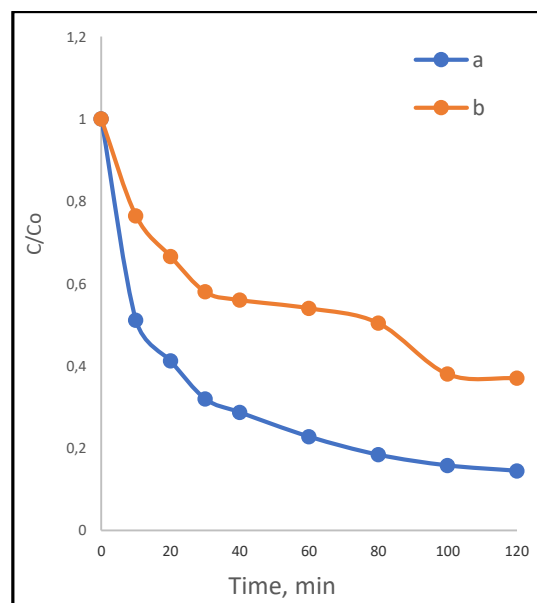**Figure 9.** T.N.T. adsorption on nickel oxide nanoparticle calcined at different time for one hr. (a) and two hr. (b)

Figure 10. T.N.T. adsorption on copper oxide nanoparticle calcined at different time for one hr. (a) and two hr. (b)

3.6. Adsorption kinetics

Adsorption kinetics was investigated for a better understanding of the mechanism of adsorption. In the present study, the adsorption data of T.N.T. by Cu-oxide and Ni-Oxide at different time intervals were analyzed by the pseudo-first-order kinetic pseudo-second-order kinetic models (Eqs. (2, 3). The two adsorption kinetic models used in this study are first-order [49] and second-order equations [50] developed by Cuevas-Villanueva et al. [51]. The first-order equation is expressed as follows (Eq. (2)):

$$ln(q_e - q_t) = Lnq_e \tag{2}$$

The second-order equation is expressed as follows (Eq. (3)):

$$\frac{t}{q_t} = \frac{1}{K_{2nd}q_e^2} + \frac{t}{q_e} \tag{3}$$

Where k_{1st} and k_{2nd} are the rates constant of first-order and second-order reaction, respectively, q_e and q_t denote the amount of adsorption at equilibrium and at time t. Kinetic parameters of these models were calculated from the slope and the intercept of the linear plots of ln $(q_e - q_t)$ vs. t for the first-order kinetic model and t/qt vs. t for second-order kinetic. The kinetics parameters' values are tabulated in Table 2, along with the corresponding linear regression correlation coefficient [52-55]. The linear plots obtained for the first-order and second-order equation are shown graphically in Figs. 11 - 14.

Table 2. The values of the kinetics parameters.

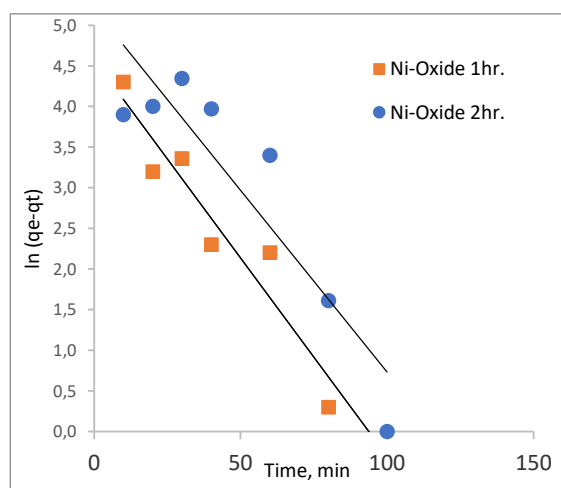| TNT concentration, (mg /L)	Nano-adsorbents	Pseudo-first-order model			Pseudo-second-order model		
		$k_1(min^{-1})$	$q_e(mg\ g^{-1})$	R^2	$k_2(g\ mg^{-1}min^{-1})$	$q_e(mg\ g^{-1})$	R^2
100	Ni-Oxide (Calc. 1hr.)	0.0488	9.695	0.95	2.4 10⁻⁵	20.41	0.98
	Ni-Oxide (Calc.	0.0447	18.193	0.83	1.17 10⁻⁵	33.3	0.99
	Cu-Oxide (Calc. 1hr.)	0.0287	11.596	0.90	2.29 10⁻³	24.45	0.99
	Cu-Oxide (Calc. 2 hr.)	0.023	10.927	0.81	1.13 10⁻³	68.03	0.96

Figure 11. Pseudo-first-order linear plots for the Adsorption of T.N.T. onto Ni-oxide calcined at 1 hr. (a) and 2 hr (b)
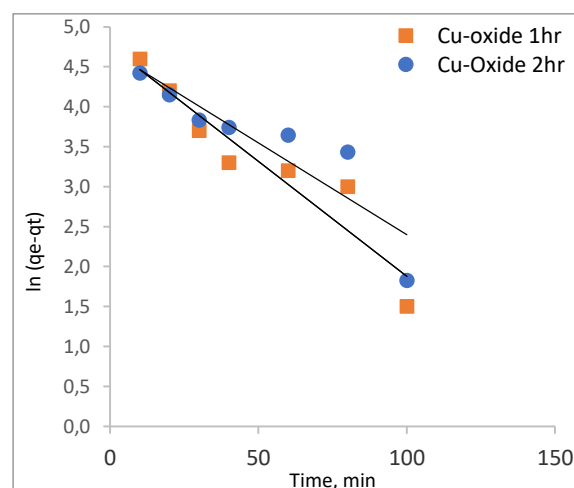

Figure 12. Pseudo-first-order linear plots for the Adsorption of T.N.T. onto Cu-oxide calcined at   1 hr.(a) and 2 hr (b)
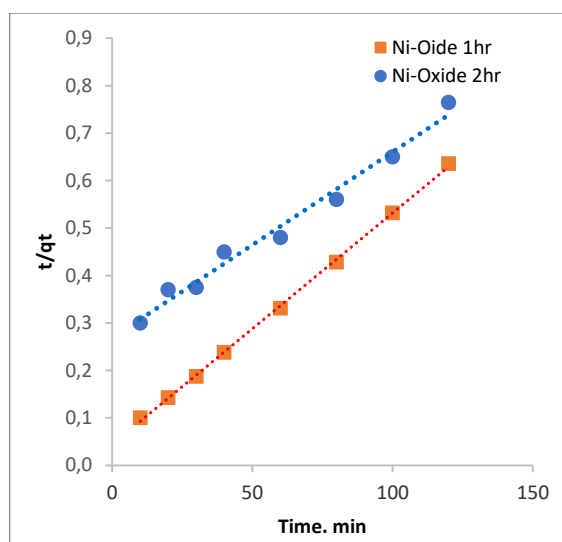
Figure 13. Pseudo-second-order linear plots for the Adsorption of T.N.T. onto Ni-oxide calcined at 1 hr. (a) and 2hr (b)
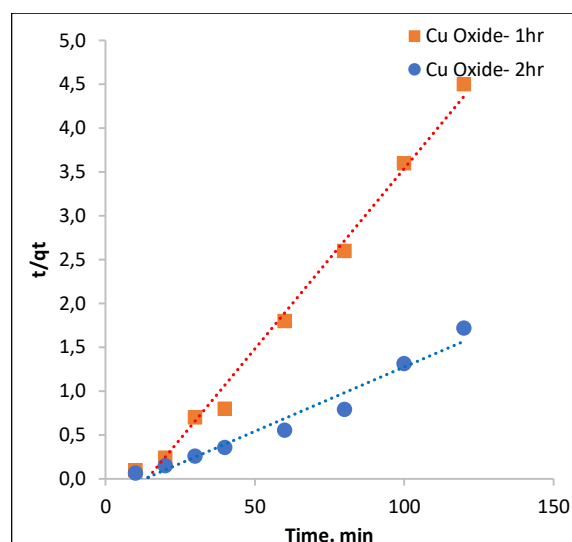

Figure 14. Pseudo- second -order linear plots for the adsorption of T.N.T. onto Cu-oxide calcined at 1 hr. (a) and 2 hr (b)

It is evident from Table 2 that the linear plot of the pseudo-second-order model gave a higher correlation coefficient for nickel oxide (R^2) value of 0.98, 0.99 as compared to that of the pseudo-first-order model 0.95, 0.83 for one and two hours, respectively. Also, the correlation coefficient for copper oxide (R^2) value of 0.99, 0.96 as compared to that of the pseudo-first-order model 0.90, 0.81 for one and two hours, respectively. This result suggested that the kinetics of T.N.T. adsorption onto metal oxide nanoparticles confirmed the pseudo-second-order model, indicating that the diffusion of the T.N.T. molecules principally controlled the overall adsorption rate into the porous system of metal oxide nanoparticles.

3.7. Reusability of the prepared adsorbents

Reusability or recycling is a significant benefit of the adsorbent for removing different contaminants due to the lower cost. Successive adsorption-desorption cycling experiments were performed to evaluate the reusability of NiO and CuO. Fig.15 shows that the removal percentage of T.N.T. after one hour were 90 % and 77% by NiO and CuO, respectively, during the first cycle and almost unaltered after five recycling runs, remaining the same percentage. These results indicated that the NiO and CuO had been reused for five cycles at a commercial scale level to lower the adsorbing materials' cost.

Figure 15. Reusability of NiO and CuO nanoadsorbents

4. Conclusion

NiO and CuO nanoparticles were prepared by the microemulsion method and evaluated as nano adsorbents to remove T.N.T. from an aqueous solution. Nano-sized nickel oxides have been successfully synthesized in cetyl trimethyl ammonium bromide/n-hexane/n-butanol/water reverse microemulsion, by fixed of surfactant, oil, and water in the microemulsion, the mixing method as well as different time of calcination temperature (1, 2 hours.). The prepared nanoparticles were

characterized by X-ray diffraction (XRD), transmission electron microscopy (T.E.M.), Electron Spin Resonance (E.S.R.), and Specific Surface Area (S.S.A.). The T.N.T. adsorption onto NiO was higher than that onto CuO, probably due to the larger surface area and pore diameter, which increase the number of active centers on the adsorbent surface high effective adsorption between nanometal oxide prepared and T.N.T. The pseudo-first-order reaction model followed the adsorption reaction of T.N.T. by the prepared adsorbents.

References

1. N.A. Khan, S.U. Khan, S. Ahmed, I.H. Farooqi, A. Dhingra, A. Hussain and F. Changani, Applications of nanotechnology in water and wastewater treatment, Water Research, **2019**, 47,3931–3946.
2. S. Pandey, A comprehensive review on recent developments in bentonite-based materials used as adsorbents for wastewater treatment, Journal of Molecular Liquids, **2017**, 241, 1091–1113.
3. N.A. Khan, S.U. Khan, S. Ahmed, I.H. Farooqi, M. Yousefi, A.A. Mohammadi, F. Changani, Recent trends in disposal and treatment technologies of emerging-pollutants–A critical review, TrAC Trends Anal Chem., **2020**, 122.
4. K.S. Ro, A. Venugopal, D.D. Adrian, D. Constant, K. Qaisi, K.T. Valsaraj, L.J. Thibodeaux, D. Roy, Solubility of 2,4,6-trinitrotoluene (TNT) in water, Chem. Eng. Data., **1996**, 41, 758–761.
5. J.D. Nijs, M. Frank, Assessment of technologies for disposing explosive waste, J. Hazard. Mater., **2002**, 90, 137–153.
6. J.C. Pennington, J.M. Brannon, Environmental fate of explosives, Thermochim. Acta., **2002**, 384, 163–172.
7. J.L. Conder, T.W. La Point, J.A. Steevens, G.R. Lotufo, Recommendations for the assessment of T.N.T. toxicity in sediments, Environ. Toxicol. Chem., **2004**, 23, 141–149.
8. M. Ikram, S. Ali, M. Aqeel, A. Ul-Hamid, M. Imrand, J. Haider, A.Haider, A. Shahbaz, S. Ali, Reduced graphene oxide nanosheets doped by Cu with highly efficient visible-light photocatalytic behavior, Journal of Alloys and Compounds, **2020**, 837, 155588.
9. M. Ikram, A. Raza, M. Imran, A. Ul-Hamid, A. Shahbaz and S. Ali, Hydrothermal Synthesis of Silver Decorated Reduced Graphene Oxide (rGO) Nanoflakes with Effective Photocatalytic Activity for Wastewater Treatment, Nano scale Research Letters, **2020**, 15, 95.
10. J. Hassan, M. Ikram, A. Ul-Hamid, M. Imran, M. Aqeel and S. Ali, Application of Chemically Exfoliated Boron Nitride Nanosheets Doped with Co to Remove Organic Pollutants Rapidly from Textile Water, Nanoscale Research Letters, **2020**, 15, 75.
11. A. Raza, M. Ikram, M. Aqeel, M. Imran, A. Ul-Hamid, K.N. Riaz, S. Ali, Enhanced industrial dye degradation using Co-doped in chemically exfoliated MoS2 nanosheets, Applied Nanoscience, **2020**, 10, 1535-1544.
12. M. Ikram, E. Umar, A. Raza, A. Haider, S. Naz, A. Ul-Hamid, J. Haider, I. Shahzadi, J. Hassan and S. Alic, Dye degradation performance, bactericidal behavior and molecular docking analysis of Cu-doped TiO_2 nanoparticles, R.S.C. Adv., **2020**, 10, 24215.
13. M. krama, S. Ali, M. Aqeel, A. Ul-Hamid, M. Imran, J. Haider, A. Haider, A. Shahbaz, S. Ali, Reduced graphene oxide nanosheets doped by Cu with highly efficient visible-light photocatalytic behavior, Journal of Alloys and Compounds, **2020**, 837, 155588.
14. S. Pandey, J. Yeon Do, J. Kim, M. Kang, Fast and highly efficient catalytic degradation of dyes using κ-carrageenan stabilized silver nanoparticles nanocatalyst, Carbohydrate polymers, **2020**, 230, 11559.
15. S. Pandey, J. Yeon Do, J. Kim, M. Kang, Fast and highly efficient removal of dye from aqueous solution using natural locust bean gum-based hydrogels adsorbent, International Journal of Biological Macromolecules, **2020**, 143, 60-75.
16. S.G. Mohammad, S.M. Ahmed, A.E. Amr and A.H. Kamel, Porous Activated Carbon from Lignocellulosic Agricultural Waste for the Removal of Acetampirid Pesticide from Aqueous Solutions, Molecules, **2020**, 25, 2339
17. Z.G. Gök, M.İna, M. Yiğitoğlu, Hacettepe Effective Degradation of 2,4,6-Trinitrotoluene (T.N.T.) with a Bacterial Consortium Developed from High TNT-degrading Bacteria Isolated from TNT-contaminated Soil, J. Biol. & Chem., **2018**, 46, 445-455.
18. S.M. Solyman, S. Shaban, S. Morsy, A.Y. El-Naggar, A.M. Badawi, S.M. Ahmed, Alkaline Hydrolysis of T.N.T. in Micellar System, Journal of Dispersion Science and Technology, **2011**, 32, 731–736.
19. A.M. Badaw, S.A. Shaban, S.M. Ahmed, S.M. Morsy and A.Y. El-Naggar, Kinetics of T.N.T. Degradation in The Presence of Zero Valent Iron Nanocatalyst, Egypt. J. Chem., **2012**, 55, 339–353.
20. X. Zhang, Y. Lin, X. Shan, Z. Chen, Degradation of 2,4,6-trinitrotoluene (T.N.T.) from explosive wastewater using nanoscale zero-valent iron, Chemical Engineering Journal, **2010**, 158, 566–570.

21. S.A. Shaban, A.M. Badawi, S.L. Sheltawy, M.M. ELShahid, Degradation of T.N.T. from aqueous solution using catalytic liquid, Int. J. Chem. Sci., **2014**, 12, 495-507.

22. A.M. Badawi, S.M, Ahmed, S.A. Shaban, S.M. Morsy, Nanotechnology: the next revolution for wastewater treatment (T.N.T. contaminate), Desalination and Water Treatment, **2012**, 40, 1–6.

23. S.M. Ahmed, S.A. Shaban, D.S. El-Desouki, N.K. Aboul-Gheit, S.M. Abdel-Azim, Photocatalytic degradation of T.N.T. in wastewater using Fe-doped TiO₂ nanoparticles, Desalination and Water Treatment, **2018**, 104, 241–249.

24. T. Guerra, I.B. Jr, Adsorption of Trinitrotoluene on a MgO Surface Including Surface Relaxation Effects, Journal of Chemistry, **2013**, 1-8.

25. I. Bharti, A.K. Khurana, A. Shaw, J.M. Saxena, P. Khurana, K. Rai, Removal of Trinitrotoluene with Nano Zerovalent Iron Impregnated Graphene Oxide, Water Air Soil Pollut., **2018**, 229, 17.

26. P. Hu, Y. Zhang, K. Tong, F. Wei, Q. An, X. Wang, P.K. Chu, F. Lv, Removal of organic pollutants from red water by magnetic-activated coke, Desalination and Water Treatment, **2015**, 54, 2710-2722.

27. M.T. Raad, M. Kassir, W. El Khatib, M. Issa, A. Hijazi, H. Bazzi, A comparative adsorption study of trinitrotoluene onto graphene oxide, reduced graphene oxide and reduced graphene oxide coated silica nanoparticles through equilibrium, kinetic and thermodynamic modeling, Graphene Technol, **2017**, 2, 63-73.

28. J. Hassan, M. Ikram, A. Ul-Hamid, M. Imran, M. Aqeel, S. Ali, Application of Chemically Exfoliated Boron Nitride Nanosheets Doped with Co to Remove Organic Pollutants Rapidly from Textile, Water Nanoscale Research Letters, **2020**, 15, 75.

29. M. Ikram, M.I. Khan, A. Raza, M. Imran, A. Ul-Hamid, S. Ali, Outstanding performance of silver-decorated MoS2 nanopetals used as nanocatalyst for synthetic dye degradation, Physica E: Low-dimensional Systems and Nanostructures, **2020**, 124, 114246.

30. J. Suárez-Cerda, H. Espinoza-Gómez, G. Alonso-Núñez, I.A. Rivero, Y. Gochi-Ponce, L.Z. Flores-López, A green synthesis of copper nanoparticles using native cyclodextrins as stabilizing agents, Journal of Saudi Chemical Society, **2017**, 21, 341–348.

31. N. Sebeia, M. Jabli, A. Ghith, T.A. Saleh, Eco-friendly synthesis of Cynomorium coccineum extract for controlled production of copper nanoparticles for sorption of methylene blue dye, Arabian Journal of Chemistry, **2020**, 13, 4263–4274.

32. M. Rashad, H. A. Al-Aoh, Promising adsorption studies of bromophenol blue using copper oxide nanoparticles, Desalination and Water Treatment, **2019**, 139, 360–368.

33. K.H. Hassan, A.A. Jarullah, S.K. Saadi, synthesis of copper oxide nanoparticle as an adsorbent for removal of Cd (II) and Ni (II) ions from binary system, International Journal of Applied Environmental Sciences, **2017**, 12, 1841–1861.

34. R. Hosseini, M.H. Sayadi, H. Shekari, Adsorption of nickel and chromium from aqueous solutions using copper oxide nanoparticles: Adsorption isotherms, kinetic modeling, and thermodynamic studies, Avicenna Journal of Environmental Health Engineering, **2019**, 6, 1-9.

35. A. Phasuk, S. Srisantitham, T. Tuntulani, W. Anutrasakda, Facile synthesis of magnetic hydroxyapatite-supported nickel oxide nanocomposite and its dye adsorption characteristics, adsorption, **2017**, 24, 157–167.

36. G. Bai, H. Dai, J. Deng, Y. Liu, W. Qiu, Z. Zhao, X. Li, H. Yang, The microemulsion preparation and high catalytic performance of mesoporous NiO nanorods and nanocubes for toluene combustion, Chemical Engineering Journal, **2013**, 219, 200-208.

37. Y. Dehmani, S. Abouarnadasse, Study of the adsorbent properties of nickel oxide for phenol depollution, Arabian Journal of Chemistry, **2020**, 5312-5325.

38. Y. Zheng, B. Zhu, H. Chen, W. You, C. Jiang, J. Yu, Hierarchical flower-like nickel (II) oxide microspheres with a high adsorption capacity of Congo red in water, J. Colloid Interface Sci., **2017**, 504, 688–696.

39. H. A. Al-Aoh, Adsorption performances of nickel oxide nanoparticles (NiO N.P.s) towards bromophenol blue dye (B.B.), Desalination and Water Treatment, **2018**, 110, 229–238.

40. W.T. Yao, S.H. Yu, Y. Zhou, Formation of uniform CuO nanorods by spontaneous aggregation: selective synthesis of CuO, Cu₂O, and Cu nanoparticles solid-liquid phase arc discharge process, J. Phys. Chem. B, **2005**, 109, 14011–14016.

41. R. Ahmadi, A. Razzaghian, Z. Eivazi, K. Shahidi, Synthesis of Cu-CuO and Cu-Cu₂O Nanoparticles via Electro-Explosion of Wire Method, Int. J. Nanosci. Nanotechnol., **2018**, 4, 93-99.

42. S.J. Brunauer, L. S.Deming, W. Deming, E.Teller, On a Theory of the van der Waals Adsorption of Gases, Journal of American Chemical Society, **1940**, 62, 1723-1732.

43. J.H. de Boer, E.P. Everette, F.S. Stone, Eds, The structure and properties of porous materials. Butterworths, (London), **1985**, 68.

44. A.M. Mahmoud, F.A. Ibrahim, S.A. Shaban, N.A. Youssef, adsorption of heavy metal ion from aqueous solution by nickel oxide nanocatalyst prepared by different methods, Egyptian Journal of Petroleum, **2015**, 24, 27–35.

45. F.Y.A. El-Kady, M.G. Abd El Wahed, S. Shaban, A.O. Abo El Naga, Hydrotreating of heavy gas oil using CoMo/γ-Al₂O₃ catalyst prepared by equilibrium deposition filtration, J. Fuel, **2010**, 89, 3193–3206.

46. M. Rubinstein, R.H. Kodama, S.A. Makhlouf, Electron spin resonance study of NiO antiferromagnetic nanoparticles, Journal of Magnetism and Magnetic Materials, **2001**, 234, 289-293

47. F. Amano, T. Tanaka, T. Funabiki, Auto-reduction of Cu(II) species supported on Al_2O_3 to Cu(I) by Thermo vacuum treatment, J. Mol. Catal. A, **2004**, 221, 89-95.

48. F. Amano, S. Suzuki, T. Yamamoto, T. Tanaka, One-electron reducibility of isolated copper oxide on alumina for selective NO–C.O. reaction, applied catalysis B: Environmental, **2006**, 64, 282-289.

49. Y.S. Ho, G. McKay, Pseudo-second order model for sorption processes, Process Biochemistry, **1999**, 34, 451-465.

50. Y.S. Ho, G. McKay, Sorption of dye from aqueous solution by peat, Chemical Engineering Journal, **1998**, 70, 115-124.

51. R.A.-Cuevas-Villanueva, A.R. Hidalgo-Vázquez, C. de Jesús, Cortés Penagos, R. Cortés-Martínez, Thermodynamic, kinetic, and equilibrium parameters for the removal of lead and cadmium from aqueous solutions with calcium alginate beads, Scientific. World J., **2014**, 1–9

52. R.O. Abo El Naga, S.A. Shaban, F.Y. El Kady, Metal-organicframework-derived nitrogen-doped nanoporous carbon as an efficient adsorbent for methyl orange removal from aqueous solution, Journal of the Taiwan Institute of Chemical Engineers, **2018**, 93, 363–373.

53. N.F Nejad, E. Shams, M.K. Amini, J.C. Bennett, Synthesis of magnetic mesoporous carbon and its application for adsorption of dibenzothiophene, Fuel Process. Technol., **2013**, 106, 376.

54. B.H. Hameed, A.A. Rahman, Removal of phenol from aqueous solutions by adsorption onto activated carbon prepared from biomass material, J. Hazard. Mater., **2008**, 160, 576.

55. N.A. Youssef, S.A. Shaban, F.A. Ibrahim, A.M. Mahmoud, Preparation of nano-Fe_2O_3 particles and evaluation of their catalytic activity in Adsorption of Pb (II), Mn (II) and Zn(II) from aqueous solution, Desalination and Water Treatment, **2017**, 69, 284–293.